ELSEVIER

Surface Science 305 (1994) 348–352

surface science

Transverse magnetic focusing and the dispersion of GaAs 2D holes at (311)A heterojunctions

J.J. Heremans *, M.B. Santos, M. Shayegan

Department of Electrical Engineering, Princeton University, Princeton, NJ 08544, USA

(Received 20 April 1993; accepted for publication 3 May 1993)

Abstract

We report transverse magnetic focusing experiments on two-dimensional hole systems confined in square and triangular quantum wells grown on (311)A GaAs substrates. The focusing barriers are oriented along different crystallographic directions and allow us to derive the constant energy contours in k-space. The results indicate a nearly elliptical shape for these contours which we interpret in light of a lateral surface superlattice induced by corrugations at the heterojunction.

The use of transverse magnetic focusing (TMF) to determine the dimension and shape of Fermi surfaces was proposed by Tsoi, and subsequently was demonstrated in metals such as Bi, Sb, W, Cu and Ag [1]. Both the periodicity in magnetic field and the shape of the focusing singularities reflect the size and geometry of the momentum space orbit. TMF was also realized in two-dimensional electron systems at GaAs/AlGaAs heterojunctions, although here the circular Fermi surface cross-sections render the focusing spectra particularly simple [2–4]. Recently, TMF was achieved [5] in two-dimensional hole systems (2DHSs) at GaAs/AlGaAs heterojunctions, where the more intricate valence band structure of GaAs can display a subset of the variety of focusing spectra found in metals. Observation of TMF in 2DHSs was made possible by recent advances in the growth of p-type heterostructures and quantum wells: molecular beam epitaxy (MBE) on the (311)A plane of the GaAs/AlGaAs system, and using Si as an acceptor dopant, has brought about a substantial improvement in the quality and mobility of the confined 2DHSs [5,6]. In this work we present a study of the directional dependence of TMF spectra taken on 2DHSs in triangular as well as square GaAs wells grown on (311)A substrates, and address the implications the experimental results bear on the in-plane energy versus wave vector dispersion relations of these systems.

TMF is achieved by drawing a current through one narrow opening (injector) and recording the voltage induced in a second opening (collector) separated from the injector by a focusing barrier of length L, as a function of a perpendicular magnetic field, B (lower part of Fig. 1). In a semi-classical model [7], under a magnetic field, the path in k-space coincides with the constant energy contours; in this case the contour defined

* Corresponding author.

SSDI 0039-6028(93)E0625-5

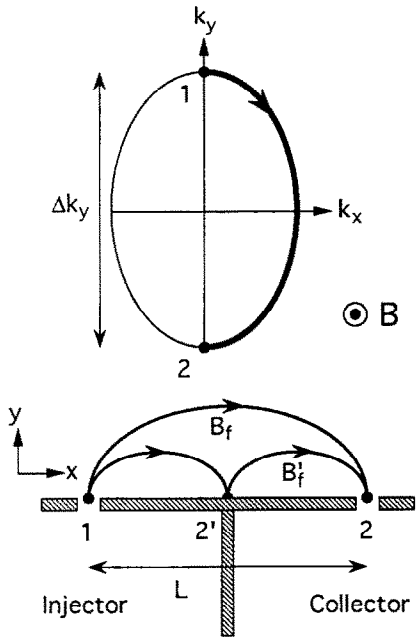

Fig. 1. Correspondence in the semi-classical model between hole paths in k-space (upper figure) and in real space (lower figure; the focusing barrier is indicated by the hatched area): the orbit 1–2 in k-space leads to the real space orbit 1–2 at field B_f, 1–2′ at field $B_f' = 2B_f$. The first focusing peak occurs at B_f, the second at B_f'. In the semi-classical model we have $B_f = (\hbar/eL)\Delta k_y$.

by the Fermi energy E_F (Fig. 1). To this corresponds a path in real space of the same shape, but rotated by $\pi/2$ and scaled by $1/B$. A chord of the real space orbit fits an integer number of times in L at those B-values where focusing peaks appear. The periodicity B_f of the signal can then be related to the k-space dimension Δk: $B_f = (\hbar/eL)\Delta k$. Hence, the experimental value of B_f should yield the value of Δk in the direction perpendicular to the focusing barrier. Orienting the barrier along different directions yields points on the constant energy contour at E_F (the Fermi surface, FS).

The sample growth on GaAs(311)A surfaces by MBE has been described elsewhere [6]. Briefly, 2DHSs were formed in both triangular and square wells. An anisotropy in the mobility μ is a consistent feature of all our samples: along [$\bar{2}$33] a higher μ is found than along [01$\bar{1}$]. The ratio of these μ is sample and density dependent, and varies between 1.5 and 3. The triangular well was realized at a single $Al_{0.35}Ga_{0.65}As/GaAs$ interface, separated from the Si dopant layer by a 210 Å spacer. For unprocessed samples of this type, typical sheet densities (p) and [$\bar{2}$33] mobilities (μ_h) were $p = 2.7 \times 10^{15}$ m^{-2} and $\mu_h = 31$ m^2/V · s, respectively. The square well samples consisted of a 150 Å wide GaAs layer, flanked on both sides by undoped $Al_{0.30}Ga_{0.70}As$ spacers and Si dopant layers. Spacers in this case were either 450 Å (unprocessed $p = 3.3 \times 10^{15}$ m^{-2} and $\mu_h = 120$ m^2/V · s) or 325 Å (unprocessed $p = 4.5 \times 10^{15}$ m^{-2} and $\mu_h = 50$ m^2/V · s). Experimental data from all these systems exhibited qualitatively similar behavior; in this paper we concentrate on data for a square well sample with 450 Å spacers.

The focusing barriers, each of equal length ($L = 3$ to 6 μm), were positioned adjacent to each other in a quarter circle, along 5 crystallographic directions ranging from [$\bar{2}$33] to [01$\bar{1}$]. In this arrangement each constriction serves in turn as collector for one barrier and as injector for the neighboring barrier (Fig. 2). Lithographic constriction widths were 0.8 μm. The TMF patterns were defined by wet etching, employing two different etchants: an $H_2SO_4 : H_2O_2 : H_2O$ solution which yielded constrictions with beveled side walls for barriers parallel to [01$\bar{1}$], and a more isotropically etching $H_3PO_4 : H_2O_2 : H_2O$ solution. Using the latter, no beveling was noticed. Experimental results coincide for both cases. Also, the etch remained shallow and did not reach the 2DHSs. Thus intrusion of possible geometric etching effects in the observed focusing spectra is unlikely. Finally, a front gate was deposited over all active areas, permitting us to modify p and hence E_F. We determined p from the transverse magnetoresistance of a nearby Hall bar. The TMF measurements were performed at 0.45 K in a 4-terminal geometry, using a low frequency lock-in technique (more details can be found in Ref. [5]).

Fig. 3 shows typical TMF spectra, plotted as collector voltage normalized by injector current versus B (relevant parameters are included in the figure). Up to 5 periodic focusing peaks appear on an up-going slope for one polarity of B, while the reverse polarity yields a flat trace. As the

focusing barrier sweeps through the 5 orientations from [$\bar{2}33$] to [$01\bar{1}$], the focusing spectra change in shape and periodicity B_f, the latter reaching the highest value for a barrier along [$\bar{2}33$]. This increase in B_f and variability in peak shapes was a consistent feature in all samples.

Fig. 4 shows a polar plot of the experimental B_f of Fig. 3 converted to $\Delta k/2$ values for the different orientations. Also shown are such polar plots for two other p for the same sample (p was varied via the front gate). Each of these represents one quarter of the FS at different E_F in k-space. The inset compares one of our experimental contours with the Fermi circle that would be obtained for the same p assuming an isotropic dispersion. At a same p, the two contours should, of course, enclose the same area, $S_k = 2\pi^2 p$. The FS derived from the TMF data exhibits a marked elongation along the [$01\bar{1}$] direction, while along [$\bar{2}33$] the dimensions are correspondingly shortened, in accordance with the requirement of preservation of the area S_k. The experimental error in our data stems mostly from the precision

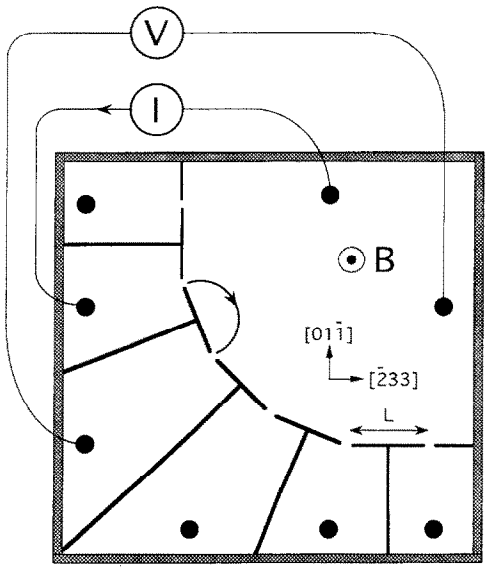

Fig. 2. Schematic representation of the sample geometry and 4-terminal measurement setup. The T-shaped focusing barriers are wet etched on the 2DHS, arranged in a quarter circle along different crystallographic orientations. Ohmic voltage and current contacts are represented by dots. The magnetic field is applied perpendicular to the sample plane.

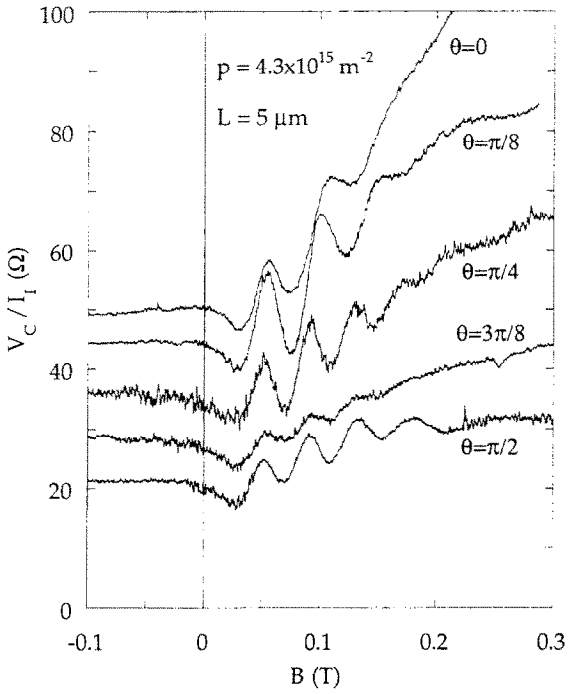

Fig. 3. TMF spectra for different orientations of the focusing barrier (collector voltage V_C normalized by injector current I_I). The angle between the focusing barrier and the [$\bar{2}33$] direction is indicated by θ. The spectra have been shifted up for clarity: $\theta = 3\pi/8$ by 5 Ω; $\theta = \pi/4$ by 10 Ω; $\theta = \pi/8$ by 15 Ω; $\theta = 0$ by 20 Ω.

to which we can ascertain the focusing peak positions, rather than from lithographic deviations and we estimate it at about 7%. For the data of Figs. 3 and 4 this error can account for the discrepancy between S_k calculated from p and from the experimental FS. The distinct near-elliptical shape of the FS constitutes a common property of all samples investigated and, in the light of the semi-classical model, originates from the underlying dispersion of the 2DHS on GaAs(311)A surfaces, as we will discuss below.

The dispersion relations for the valence band of GaAs quantum wells at the (311)A surface have been previously studied theoretically [8], largely confirming resonant magnetotunneling spectroscopy experiments [9]. Higher subbands apparently display considerable nonparabolicity and anisotropy, while the lowest, heavy hole, subband remains quite free-hole-like up to high den-

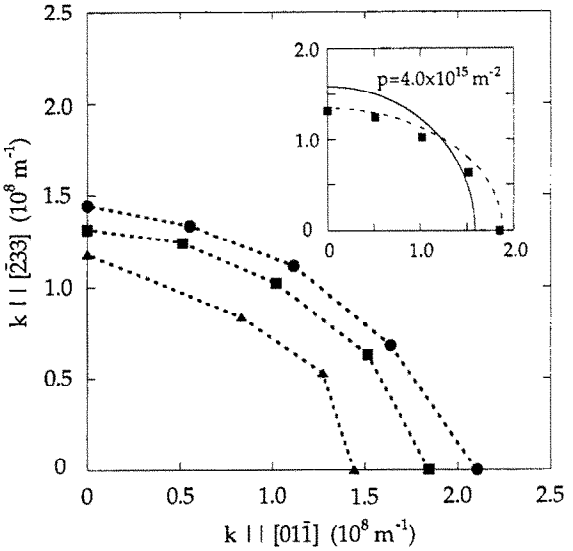

Fig. 4. Constant energy contours in k-space determined from TMF data at varying p (circles: $p = 4.3\times10^{15}$ m^{-2}; squares: $p = 4.0\times10^{15}$ m^{-2}; triangles: $p = 3.1\times10^{15}$ m^{-2}). Inset: comparison between experimental points (squares), isotropic Fermi circle (solid curve) and Kronig–Penney calculation (dashed curve) for $p = 4.0\times10^{15}$ m^{-2}.

sities. Therefore in our samples, where only the lowest subband is occupied, the dispersion anisotropy (Fig. 4) and also the mobility anisotropy mentioned earlier are puzzling.

However, MBE on GaAs(311)A substrates has been reported [10] to induce interface corrugations along [$\bar{2}$33] and the transport anisotropy likely stems from this morphology. The corrugations, with a period of 32 Å, give rise to a one-dimensional lateral superlattice (LSL) along [01$\bar{1}$] for holes confined to a GaAs well [11]. Such a LSL modifies the dispersion along [01$\bar{1}$] while along [$\bar{2}$33] the dispersion should be unchanged from its free-hole form [12]. A straightforward Kronig–Penney calculation indicates that the LSL produces an elongation of the FS along the [01$\bar{1}$] direction compared to [$\bar{2}$33]. This is consistent with our TMF experiments. Let us note that for E_F values typically achieved in our 2DHSs, k_F amounts to about 1/10 of the Brillouin zone induced by this LSL. To account for the distortion observed in our data at these p, the LSL potential amplitude needed is about 200 to 300 meV, the value being sample dependent as expected for a growth related phenomenon. The FS obtained from the Kronig–Penney model (assuming for simplicity square barriers of width equal to half the period and height 300 meV) is plotted in the inset of Fig. 4. While a more realistic potential profile would be desirable, we feel that the qualitative features of the experimental data are well reproduced.

In conclusion, TMF employing a geometry of adjacent barriers in varying crystallographic directions enabled us to map out the constant energy contours in k-space for the heavy hole band of a 2DHS on the (311)A plane of GaAs. We interpret the data in a semi-classical model. Although the dispersion for the heavy hole band on (311)A surfaces is expected to be quite isotropic, nearly elliptical contours were deduced, with their long axis along the [01$\bar{1}$] orientation. We trace this shape back to the existence of a lateral superlattice, generated by growth induced corrugations along the [$\bar{2}$33] direction.

We thank K. Hirakawa for helpful discussions. This work was supported by the National Science Foundation, the Army Research Office and the IBM Corporation. The authors are affiliated with the Advanced Technology Center in Photonics and Opto-Electronic Materials established at Princeton University by the State of New Jersey.

1. References

[1] V.S. Tsoi, JETP Lett. 19 (1974) 70;
V.S. Tsoi, JETP Lett. 22 (1975) 197;
S.A. Korzh, Sov. Phys.-JETP 41 (1975) 70;
V.S. Tsoi and I.I. Razgonov, Sov. Phys.-JETP 47 (1978) 597.

[2] H. van Houten, C.W.J. Beenakker, J.G. Williamson, M.E.I. Broeckaart, P.H.M. van Loosdrecht, B.J. van Wees, J.E. Mooij, C.T. Foxon and J.J. Harris, Phys. Rev. B 39 (1989) 8556.

[3] J. Spector, H.L. Stormer, K.W. Baldwin, L.N. Pfeiffer and K.W. West, Surf. Sci. 228 (1990) 283.

[4] K. Nakamura, D.C. Tsui, F. Nihey, H. Toyoshima and T. Itoh, Appl. Phys. Lett. 56 (1990) 385.

[5] J.J. Heremans, M.B. Santos and M. Shayegan, Appl. Phys. Lett. 61 (1992) 1652.

[6] W.I. Wang, E.E. Mendez, Y. Iye, B. Lee, M.H. Kim and G.E. Stillman, J. Appl. Phys. 60 (1986) 1834;

A.G. Davies, J.E.F. Frost, D.A. Ritchie, D.C. Peacock, R. Newbury, E.H. Linfield, M. Pepper and G.A.C. Jones, J. Cryst. Growth 111 (1991) 318;
M.B. Santos, Y.W. Suen, M. Shayegan, Y.P. Li, L.W. Engel and D.C. Tsui, Phys. Rev. Lett. 68 (1992) 1188.

[7] Our experiments involve samples with high sheet density and relatively wide injector and collector openings, so that the Fermi wavelength (λ_F) is much smaller than the opening width (W). Therefore, as in the case of TMF in metals, a semi-classical model is appropriate. In particular, we note that the quantum interference effects, manifested as reproducible fine structure superimposed on the focusing spectra, are essentially absent in our data (c.f. van Houten et al. [2] where $\lambda_F \approx W$, and also see G. Goldoni and A. Fasolino, Phys. Rev. B 44 (1991) 8369, for a theoretical discussion of subband structure effects on TMF in 2DHSs in the quantum mechanical regime).

[8] E.C. Valadares, Phys. Rev. B 46 (1992) 3935.

[9] R.K. Hayden, E.C. Valadares, M. Henini, L. Eaves, D.K. Maude and J.C. Portal, Phys. Rev. B 46 (1992) 15586.

[10] R. Noetzel, N.N. Ledentsov, L. Daeweritz, K. Ploog and M. Hohenstein, Phys. Rev. B 45 (1992) 3507;
R. Noetzel, N.N. Ledentsov and K. Ploog, Phys. Rev. B 47 (1993) 1299.

[11] The presence of minigaps and the possibility of a LSL for 2D electrons at the vicinal Si/SiO_2 interfaces, such as (811), have been previously reported:
T. Cole, A.A. Lakhani and P.J. Stiles, Phys. Rev. Lett. 38 (1977) 722;
L.J. Sham, S.J. Allen, Jr., A. Kamgar and D.C. Tsui, Phys. Rev. Lett. 40 (1978) 472;
see also, T. Ando, A.B. Fowler and F. Stern, Rev. Mod. Phys. 54 (1982) 437.

[12] Irregularities in the periodicity or strength of the LSL's periodic potential may be responsible for the enhanced scattering and reduced mobility in the [01$\bar{1}$] direction.